# Automatic Quantitative Left Ventricular Analysis of Cine MR Images by Using Three-dimensional Information for Contour Detection[1]

Robert Jan M. van Geuns, MD, PhD
Timo Baks, MD
Ed H. B. M. Gronenschild, PhD
Jean-Paul M. M. Aben, BSc
Piotr A. Wielopolski, PhD
Filippo Cademartiri, MD, PhD
Pim J. de Feyter, MD, PhD

The purpose of this study was to evaluate an automatic boundary detection algorithm of the left ventricle on magnetic resonance (MR) short-axis images with the essential restriction of no manual corrections. The study comprised 13 patients (nine men, four women) and 12 healthy volunteers (11 men, one woman), and institutional review board approval and informed consent were obtained. The outline of the left ventricle was indicated manually on horizontal and vertical long-axis MR images. The calculated intersection points with the short-axis MR images were the basis of the automatic contour detection. Automatically derived volumes correlated highly with manually derived (short axis–based) volumes ($R^2 = 0.98$); ejection fraction (EF) and mass showed a correlation of 0.95 and 0.93, respectively. Automatic contour detection reduced interobserver variability to 0.1 mL for endocardial end-diastolic and end-systolic volumes, 1.1 mL for epicardial end-diastolic and end-systolic volumes, 0.02% for EF, and 1.1 g for mass. Thus, the algorithm enabled highly reproducible left ventricular parameters to be obtained.



[1] From the Departments of Cardiology (R.J.M.v.G., T.B., P.J.d.F.) and Radiology (R.J.M.v.G., T.B., P.A.W., F.C., P.J.d.F.), Erasmus Medical Center, Thoraxcenter Ba 585, PO Box 2040, 3000 CA Rotterdam, the Netherlands; Department of Medical Informatics, Maastricht University, Maastricht, the Netherlands (E.H.B.M.G.); and Pie Medical Imaging, Maastricht, the Netherlands (J.P.M.M.A.). Received March 21, 2005; revision requested May 12; revision received July 10; accepted July 27; final version accepted September 14. **Address correspondence to** R.J.M.v.G. (e-mail: *r.vangeuns@erasmusmc.nl*).

Accurate and reproducible assessment of left ventricular volumes and ejection fraction (EF) is essential for prognosis in patients with heart diseases and for evaluating therapeutic responses (1,2). Magnetic resonance (MR) imaging has proved to be an accurate and reproducible imaging modality for the quantitative analysis of left ventricular function (3,4). Left ventricular volume and mass, as well as regional functional parameters such as wall motion and wall thickening, are usually obtained in the true short-axis plane of the left ventricle (5–8). These short-axis views minimize partial volume effects and are perpendicular to the direction of wall motion and wall thickening.

Automatic segmentation of the left ventricle on MR images is not trivial. One of the main obstacles is caused by the transitions in gray levels across the endocardial and epicardial boundaries, which are not sharp and differ in sign (from high to low signal intensity and vice versa). Moreover, large variations in image quality at MR imaging and large variations in the shape of the left ventricle pose even more challenges for such an image-processing task. Several approaches for border recognition have been developed, which range from manual to semiautomatic and fully automatic techniques (9–19). The applied techniques range from purely data-driven (edge detection, region growing) to model-driven (model fitting) techniques.

Because of the limited or partially successful performance of the reported methods, we have developed an automatic boundary detection algorithm. The proposed algorithm does not make any anatomic assumptions and requires only a set of manually obtained epicardial contours on the two- and four-chamber MR images at end systole and end diastole as single-user input. It takes advantage of the three-dimensional information obtained from the MR imaging system in order to start the segmentation process for both endocardial and epicardial contours on all short-axis sections. An obvious benefit of such an approach is its intrinsic high reproducibility.

The purpose of our study was to evaluate an automatic boundary detection algorithm of the left ventricle on MR short-axis images with the essential restriction of no manual corrections.

**Advance in Knowledge**

- The algorithm we used allowed us to perform highly reproducible automatic measurements of left ventricular parameters.

## Materials and Methods

### Patient Selection

The study population consisted of 13 patients and 12 healthy volunteers. The patients (nine men, four women; age range, 38–78 years; mean age, 57 years) were studied for left ventricular function in a protocol on experimental cell therapy for ischemic heart failure. The volunteers (11 men, one woman; age range, 23–53 years; mean age, 30 years) reported no history of cardiac disease or current health problems. In six patients and nine volunteers, cine MR imaging was performed twice, with a time interval from 1 hour to 1 year. This resulted in a total of 40 imaging studies included in our evaluation. All patients and volunteers gave informed consent, and this study, including the protocol on experimental cell therapy, was approved by the institutional review board at Erasmus Medical Center.

### Data Acquisition

All patients and healthy volunteers were examined by using a 1.5-T whole-body MR imaging system (Sonata; Siemens, Erlangen, Germany). Cine MR imaging was performed by using an electrocardiographically triggered breath-hold steady-state free precession acquisition technique, with the subject in a supine position and a four-channel quadrature body phased-array coil placed over the thorax. Imaging parameters were as follows: 3.2/1.6 (repetition time msec/echo time msec); flip angle, 65°; temporal resolution, 47 msec; section thickness, 8 mm; section gap, 2 mm; field of view, 300 × 340 mm; and matrix size, 224 × 256. By using standard techniques to identify the major cardiac axes, two-chamber, four-chamber, and short-axis cine MR sequences were performed during breath hold in the end-expiratory phase. Typically, 11 cine breath-hold short-axis MR sections were acquired to encompass the entire left ventricle from apex to base. The number of images per cardiac cycle was dependent on the heart rate and varied between 18 and 24. The total imaging time for a complete imaging study was about 20 minutes.

### Image Analysis

All the studies were transferred to a personal computer equipped with Windows (Microsoft, Redmond, Wash) for further analysis with the current algorithm, which was implemented with the CAAS-MRV program (version 1.0; Pie Medical Imaging, Maastricht, the Netherlands). Two experienced investigators (R.J.M.v.G. and T.B., with 9 and 2 years of cardiac MR imaging experience, respectively) independently traced both the endocardial and epicardial contours manually on the short-axis views in the end-diastolic and end-systolic heart phases, which served as reference results. One observer (R.J.M.v.G) traced contours on all 40 studies and subsequently a subset of 10 studies (from the first seven patients and the first three volunteers) in order to derive the intraobserver variability. An independent second observer (T.B.) traced contours on the same subset of 10 studies to derive the interobserver vari-

**Published online**
10.1148/radiol.2401050471

**Radiology 2006;** 240:215–221

**Abbreviation:**
EF = ejection fraction

**Author contributions:**
Guarantors of integrity of entire study, R.J.M.v.G., E.H.B.M.G., J.P.M.M.A.; study concepts/study design or data acquisition or data analysis/interpretation, all authors; manuscript drafting or manuscript revision for important intellectual content, all authors; manuscript final version approval, all authors; literature research, R.J.M.v.G., E.H.B.M.G.; clinical studies, R.J.M.v.G., P.A.W.; statistical analysis, R.J.M.v.G., E.H.B.M.G.; and manuscript editing, R.J.M.v.G., T.B., E.H.B.M.G., J.P.M.M.A.

Authors stated no financial relationship to disclose.

ability. Papillary muscles and trabeculations were treated as part of the blood pool volume.

For the automatic left ventricle segmentation, a total of four epicardial contours are required—one on each of the two-chamber end-diastolic and end-systolic views and one on each of the four-chamber end-diastolic and end-systolic views. These contours can be drawn relatively quickly by indicating the valve plane by means of two points followed by the apex position. An open spline curve is then fitted through these points. Adding, adjusting, or removing points will tailor the curve to the desired shape. Typically, eight points are sufficient to indicate the epicardial wall. Again the first observer (R.J.M.v.G.) traced all 40 studies, and the second observer (T.B.) traced the same 10 studies as for the full manual analysis. By using the absolute system coordinates obtained from the MR imaging system (through the Digital Imaging and Communications in Medicine headers), the short-axis MR images can be cross-referenced with the orthogonal two- and four-chamber long-axis views, as depicted in Figure 1. This results in four intersection points of the long-axis epicardial borders with each short-axis section. A closed spline curve is automatically fitted to these points, which yields a first guess of the short-axis epicardial border.

By starting from this first guess, a segmentation algorithm is used to derive the endocardial borders on this section for all cardiac phases (18–24 phases). This algorithm draws heavily on the concept of fuzzy objects, in which image elements (pixels, voxels) exhibit a similarity or "hanging togetherness" both in geometry and in gray-scale values (20). The algorithm will properly differentiate the papillary muscles located inside the left ventricle from the blood volume. A smooth convex hull produces the final endocardial contour, which now includes the papillary muscles as part of the left ventricular volume. Guided by this endocardial contour, the epicardial contour is subsequently obtained on the basis of a radial minimum cost algorithm. This step is repeated for all short-axis sections covering the left ventricle as defined on the long-axis views. The average segmentation time is about 2 minutes with use of a 2.4-GHz Pentium IV processor (Intel, Santa Clara, Calif). Within this time, the full set of multiphase and multisection short-axis studies (typically 300 images) is segmented. We have to stress here that for the current study, no manual corrections were performed afterward.

Each endocardial and epicardial volume was computed by using the Simpson rule: It is the summation over all sections of the areas within the endocardial and epicardial contours multiplied by the section thickness (including the intersection gap). Myocardial mass was calculated by taking the difference of the end-diastolic endocardial volume and the end-diastolic epicardial volume multiplied by 1.05 g/cm$^3$, which is the standard mass for each cubic centimeter. Finally, the EF was derived by calculating the stroke volume from end-diastolic and end-systolic endocardial volumes, divided by the end-diastolic endocardial volume.

### Statistical Analysis

To assess the reliability of the automatic segmentation algorithm, the derived end-diastolic and end-systolic ventricular volumes for the endocardium and epicardium, as well as values for the EF and the myocardial mass, were compared with the manually derived values of the first observer (R.J.M.v.G.). The agreement between the manual and automatic segmentation was expressed as the mean and standard deviation of the paired differences in each data set. A two-tailed paired Student *t* test was performed to determine the statistical significance of the observed differences. A *P* value of less then .05 was considered to indicate a statistically significant difference. The percentage difference relative to the average value of the paired manual volumes was also calculated. A linear regression analysis was applied to

**Figure 1**

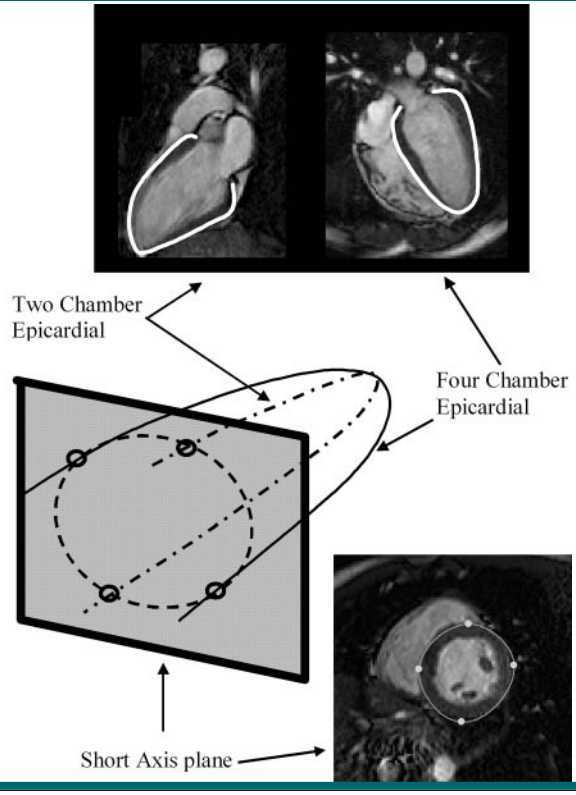


**Figure 1:** On the basis of the epicardial boundaries on the two- and four-chamber MR images, four intersection points with each short-axis MR image can be determined. A spline is fitted to these four points that subsequently starts the automatic left ventricle segmentation algorithm.

quantify the correlation between the automatic and manual volumes.

To be able to put the observed differences in perspective, we also determined the inter- and intraobserver variabilities of the measurements on the basis of a repeated manual tracing of the ventricular borders. Two comparison sets were obtained, each based on 10 MR imaging studies: measurements obtained by R.J.M.v.G. the first time versus the second time (intraobserver variability) and the averaged difference of measurements obtained by R.J.M.v.G. the first time versus T.B. and those obtained by R.J.M.v.G. the second time versus T.B. (interobserver variability).

As described, the automatic segmentation is started from manually drawn two- and four-chamber epicardial contours. To assess the reproducibility of the automatic segmentation algorithm, these contours were drawn twice by R.J.M.v.G. and independently once by T.B., all on the same 10 MR studies. An essential prerequisite for determining the reproducibility is that no manual corrections are made afterward. On the basis of the available three sets of contours, an estimate of the true reproducibility of the algorithm was derived.

In view of the small number of paired values ($n = 10$), a Wilcoxon signed rank test was applied to determine the statistically significant differences between intra- and interobserver variabilities and between observer variabilities of manual and automatic segmentation.

**Table 1**

**Intra- and Interobserver Variabilities Based on 10 Manually Drawn Contours**

| Parameter | Intraobserver Variability* | | Interobserver Variability† | |
|---|---|---|---|---|
| | Value | Percentage | Value | Percentage |
| Endocardial volume (mL) | | | | |
| End diastolic | −6.18 ± 3.63‡ | −2.57 ± 1.51 | 16.07 ± 13.90‡ | 6.46 ± 5.58§ |
| End systolic | −3.20 ± 3.96‡ | −2.07 ± 2.56 | 17.72 ± 14.85‡ | 10.61 ± 8.89§ |
| Epicardial volume (mL) | | | | |
| End diastolic | 0.46 ± 4.03 | 0.11 ± 0.97 | −15.21 ± 12.41‡ | −3.74 ± 3.05§ |
| End systolic | 4.37 ± 7.46‡ | 1.35 ± 2.30 | −15.36 ± 12.70‡ | −4.77 ± 3.95§ |
| EF (%) | −0.08 ± 2.49 | −0.20 ± 6.15 | −2.37 ± 2.53 | −5.57 ± 5.95§ |
| Mass (g) | 6.98 ± 6.83‡ | 3.82 ± 3.74 | −32.85 ± 20.54‡ | −19.76 ± 12.35§ |

Note.—Data are mean ± standard deviation.

* Difference between the second measurement minus the first measurement obtained by R.J.M.v.G.

† Averaged difference of the measurement obtained by T.B minus that obtained by R.J.M.v.G. the first time and the measurement obtained by T.B. minus that obtained by R.J.M.v.G. the second time.

‡ Statistically significant ($P < .05$).

§ Statistically significant ($P < .05$) in comparison with intraobserver variability.

**Table 2**

**Comparison of Automatic and Manual Left Ventricular Measurements**

| Parameter | Automatic Minus Manual* | | Linear Regression | Adjusted $R^{2}$† | Standard Error‡ |
|---|---|---|---|---|---|
| | Value | Percentage | | | |
| Endocardial volume | | | | | |
| End diastolic | −8.15 mL ± 11.46§ | −5.05 ± 7.10 | 0.95x + 0.33 | 0.98 | 10.86 mL |
| End systolic | −5.95 mL ± 6.34§ | −6.71 ± 7.15 | 0.98x − 4.19 | 0.99 | 6.28 mL |
| Epicardial volume | | | | | |
| End diastolic | −1.30 mL ± 17.11 | −0.42 ± 5.48 | 0.94x + 16.87 | 0.98 | 15.78 mL |
| End systolic | 12.12 mL ± 13.96§ | 5.25 ± 6.05 | 0.98x + 17.25 | 0.98 | 13.93 mL |
| EF | 1.61% ± 3.53 | 5.06 ± 13.12 | 1.00x + 1.55 | 0.95 | 3.63% |
| Mass | 7.19 g ± 15.00§ | 5.91 ± 10.52 | 0.93x + 18.93 | 0.93 | 14.76 g |

* Data are mean ± standard deviation for the difference between the automatic measurement minus the manual measurement.

† Squared adjusted multiple correlation.

‡ Standard error of the residuals.

§ Statistically significant ($P < .05$).

## Results

For the volunteers, the manual average end-diastolic volume was 125 mL ± 27 (standard deviation), and the average end-systolic volume was 49 mL ± 11. Values for EF and mass were 60% ± 6 and 124 g ± 23, respectively. These results are concordant with findings in the literature.

For the patients, the manual average end-diastolic volume was 201 mL ± 94, and average end-systolic volume was 132 mL ± 77. Values for EF and mass were 36% ± 16 and 196 g ± 62, respectively.

### Intra- and Interobserver Variabilities of Manual Volumes, EF, and Mass

For the manual measurements, there was a significant difference between the first and second measurement of the first observer (R.J.M.v.G.) for the two endocardial volumes, the end-systolic epicardial volume, and mass (Table 1). A significant difference also existed between the two observers for all measurements except for EF. There was an agreement between the two observers on a level of about 17 mL (8%) for the endocardial volumes and about 15 mL (4%) for the epicardial volumes. For EF, the level of agreement was about 2 percentage points (5%). For the myocardial mass, the intraobserver variability was about 7 g (4%), whereas the interobserver variability was much larger (approximately 33 g [20%]) because there was a systematic positive difference for endocardial volumes combined with a negative difference for epicardial volumes between the two observers. For all measurements the interobserver variability

**Figure 2**

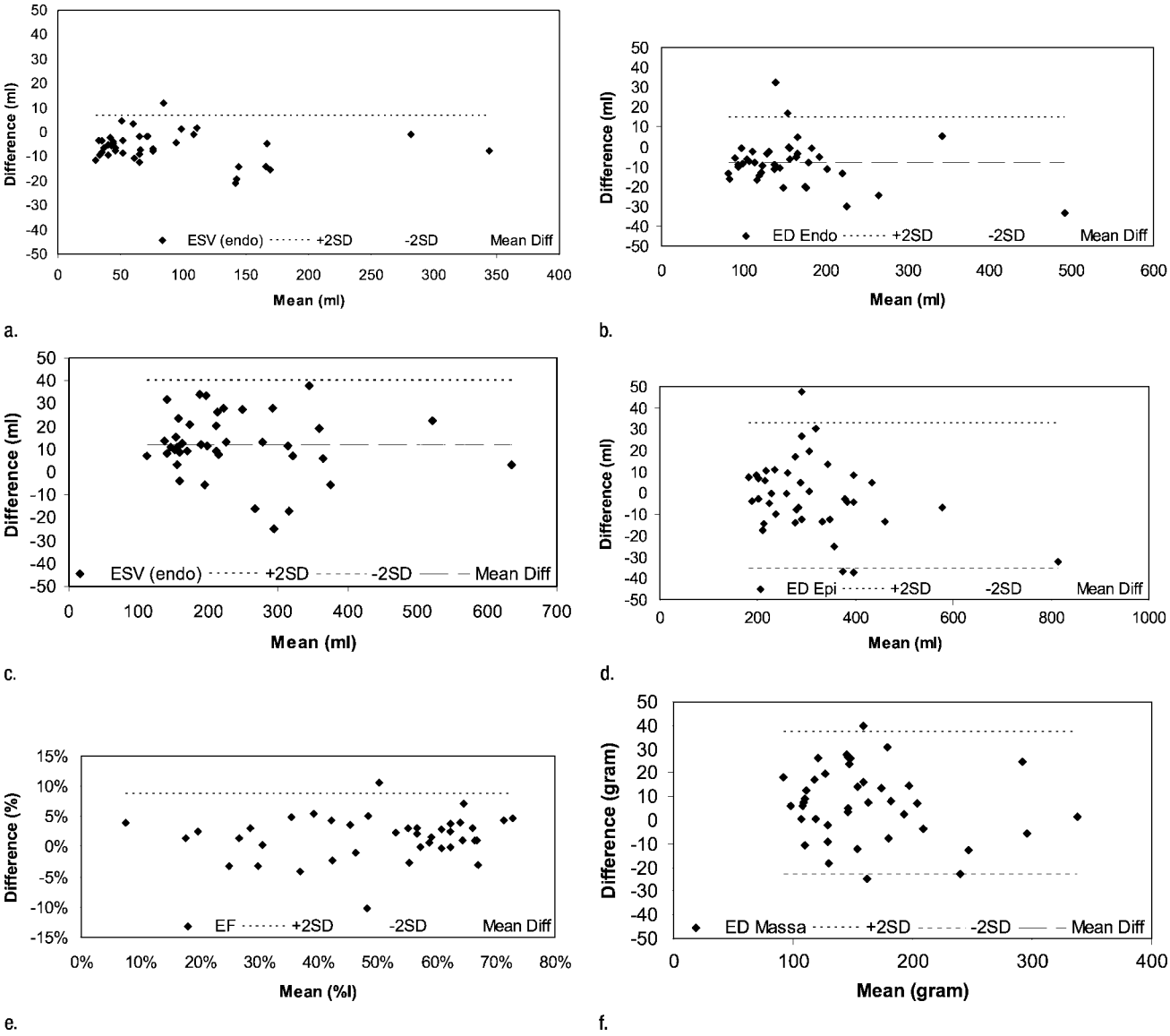


**Figure 2:** Bland-Altman plots show comparison of manually derived left ventricular volumes with automatically derived volumes. The results are presented in plots for the endocardial **(a)** end-systolic *(ESV)* and **(b)** end-diastolic *(ED)* volumes, for the epicardial **(c)** end-systolic *(ESV)* and **(d)** end-diastolic *(ED)* volumes, and for **(e)** EF and **(f)** mass. Dashed lines show respective means of the volume differences, and dotted lines indicate ± 2 standard deviations *(2SD)*.

was significantly larger than was the intraobserver variability.

### Reliability of Automatic Volumes, EF, and Mass

There was excellent agreement (squared adjusted multiple correlation, $R^2 = 0.93$–$0.99$) between the automatic and manual measurement of the left ventricular volumes, EF, and myocardial mass (Table 2). We observed a slight underestimation in the endocardial volumes of about 5% and a slight overestimation in the epicardial volume (mean, 2%), which resulted in a moderately overestimated myocardial mass (approximately 6%). The EF was also slightly overestimated in comparison with the manually derived value (about 5%). The results are comparable with the interobserver variabilities listed in Table 1 and are slightly worse than the intraobserver variabilities. The results are further detailed in Bland-Altman plots (Fig 2) showing the differences for each of the two paired measurements versus their averages.

### Reproducibility of Automatic Volumes, EF, and Mass

For the automatic contour detection, no significant differences could be observed between the first and second measurement of the first observer or

between the first and second observer (Table 3).

The reproducibility of the automatic analysis is high for the endocardial volumes; compared with the manual intra- and interobserver variabilities, it can be noticed that the average difference, as well as the standard deviation, was dramatically decreased to a level of 0.35 mL (0.20%) or less and 1.32 mL (0.61%) or less, respectively. For the epicardial volumes, EF, and myocardial mass, the reproducibility was significantly ($P < .05$) higher compared with the interobserver variabilities, whereas it was similar to the intraobserver variabilities.

## Discussion

An automatic left ventricle segmentation algorithm has been developed that requires only a set of epicardial contours on the two- and four-chamber end-diastolic and end-systolic MR sections as single-user input. In this study, no manual contour editing was performed, allowing a reliable comparison with manual measurements and a true assessment of the reproducibility of the segmentation technique.

The automatically derived endocardial and epicardial volumes highly correlate with the volumes obtained at manual analysis, although a statistically significant systematic difference is present for some measurements. Obtaining a high correlation between two measurements is more important than obtaining a small absolute difference, especially when no reference standard is available. In addition, the systematic differences are of the same order as the intra- and interobserver variabilities for the manual measurements. Also, in this respect, the automatic segmentation performed equally as well as an experienced observer.

Moreover, the reliability of the endocardial volumes is similar to those reported in literature (Table 4). It should be noted that values for the epicardial volumes are not present in any literature known to us. Usually, however, myocardial mass is reported which is implicitly dependent on both the epicardial and endocardial contours. The results for myocardial mass by using our technique without manual corrections are comparable with results obtained with techniques involving manual corrections. The summary of the results in Table 4 shows an interesting finding: In all cases but one, the endocardial volumes are underestimated in comparison with the manually derived volumes. The explanation of this deviation is not completely understood. Most likely, considerations other than those purely based on pixel gray-scale values play a role in the manual delineation of the ventricular borders by a clinician. With this in mind, there may be some room for future improvements here.

A basic requirement for any automatic algorithm is that it is highly reproducible. To assess the reproducibility, we varied the input of the algorithm by repeating the manual tracing of the long-axis contours by the same investigator (R.J.M.v.G.) and by an independent second investigator (T.B.). This resulted in a strong reduction of the intra- and interobserver variabilities from about 18 mL (10.6%) to about 0.35 mL (0.2%) for the endocardial volumes and from about 15 mL (4.8%) to about 4.5 mL (1.1%) for the epicardial volumes. Restricting the comparison to the interobserver variabilities, the reduction is even more spectacular: from about 17

**Table 3**

**Intra- and Interobserver Variabilities Based on 10 Automatically Drawn Contours**

| | Intraobserver Variability* | | Interobserver Variability† | |
|---|---|---|---|---|
| Parameter | Value | Percentage | Value | Percentage |
| Endocardial volume (mL) | | | | |
| End diastolic | −0.35 ± 1.32 | −0.16 ± 0.61‡ | −0.08 ± 0.32 | −0.04 ± 0.15‡ |
| End systolic | −0.28 ± 0.54 | −0.20 ± 0.37‡ | −0.07 ± 0.45 | −0.05 ± 0.30‡ |
| Epicardial volume (mL) | | | | |
| End diastolic | −4.53 ± 6.82 | −1.11 ± 1.68 | −1.11 ± 6.33 | −0.27 ± 1.55‡ |
| End systolic | −1.35 ± 6.77 | −0.37 ± 1.84 | −1.05 ± 9.63 | −0.29 ± 2.63‡ |
| EF (%) | −0.21 ± 0.36 | −0.52 ± 0.88‡ | −0.02 ± 0.26 | −0.05 ± 0.69‡ |
| Mass (g) | −4.38 ± 6.97 | −2.19 ± 3.49 | −1.08 ± 6.65 | −0.52 ± 3.1‡ |

Note.—Data are mean ± standard deviation.

* Difference between the second measurement minus the first measurement obtained by R.J.M.v.G.

† Averaged difference of the measurement obtained by T.B. minus that obtained by R.J.M.v.G. the first time and the measurement obtained by T.B. minus that obtained by R.J.M.v.G. the second time.

‡ Statistically significant ($P < .05$) in comparison with manual intra- or interobserver variability.

**Table 4**

**Comparison of Current Study Results and Results in the Literature**

| | | Endocardial Volume | | | |
|---|---|---|---|---|---|
| Study | Year* | End Diastolic (mL) | End Systolic (mL) | EF (%) | Mass (g) |
| van der Geest et al (10) | 1997 | −5.5 ± 9.7 | −3.6 ± 6.5 | 1.7 ± 4.1 | 7.2 ± 15.0 |
| Nachtomy et al (12) | 1998 | 15.3 ± 13.7 | −1.4 ± 7.1 | 0.85 ± 7.0 | 27.1 ± 40.6 |
| Furber et al (11) | 1998 | · · · | · · · | · · · | 8.5 ± 6.1 |
| Lalande et al (13) | 1999 | · · · | · · · | 4.7 ± 2.7 | · · · |
| Graves et al (15) | 2000 | −8.8 ± 5.3 | −2.2 ± 3.6 | −0.9 ± 3.1 | · · · |
| Young et al (14) | 2000 | 2.2 ± 4.6 | 2.3 ± 3.8 | 1.1 ± 2.5 | 1.8 ± 4.9 |
| Barkhausen et al (16) | 2001 | −4.8 ± 9.2 | −3.8 ± 6.75 | 0.5 ± 3.2 | · · · |
| Francois et al (18) | 2004 | · · · | · · · | · · · | 5.0 ± 7.2 |
| van der Geest et al (19) | 2004 | −2.9 ± 13.2 | −5.1 ± 18.9 | 0.0 ± 6.8 | −1.2 ± 14.1 |
| Current study | 2006 | −8.15 ± 11.46 | −5.95 ± 6.34 | 1.6 ± 3.5 | 7.19 ± 15.00 |

Note.—Data are mean ± standard deviation.

* Publication year of study results.

mL (8%) to less than 0.1 mL (0.05%) for the endocardial volumes and from about 15 mL (4%) to about 1.1 mL (0.3%) for the epicardial volumes. For the associated myocardial mass, the reduction is from about 33 g (20%) to about 1 g (0.5%), and for EF, the reduction is from about 2 percentage points (5%) to 0.01 percentage point (0.04%). Such a high reproducibility can be expected for the approach we took to perform an automatic segmentation. To our knowledge, this is the first time that the reproducibility of a left ventricular automatic segmentation algorithm has been assessed.

Whereas almost all techniques are based on only short-axis MR image stacks, only Graves et al (15) described a technique that makes use of the two- and four-chamber sections. A severe limitation of their method is that only endocardial contours are derived, while the epicardial contours are manually drawn. The power of our algorithm is that the epicardial contour is also automatically detected.

Additional advantages of the method of segmentation presented herein are as follows: Although the described validation has been performed only for the end-diastolic and end-systolic cardiac phases, the segmentation algorithm is able to depict the endocardial and epicardial border in all acquired cardiac phases, without any further user interaction. Furthermore, information not present on the short-axis MR images can be incorporated in the analysis. For instance, localization of the mitral valve annulus as a separator between ventricular and atrial volume is difficult on short-axis MR images and can be better defined on two- and four-chamber MR images. These images also show the motion of the annulus during cardiac motion and the delineation of the apex more clearly. Because of an improved localization of the mitral valve and the apex, it is possible to make corrections to the ventricular volume derived from the contours.

For optimal cross-referencing of the long-axis and short-axis MR acquisitions, reproducibility of the breath-hold position is important. Inconsistency in breath holding will hamper cross-referencing but will also lead to impaired image quality of the short-axis MR images, making reliable assessment of left ventricular volumes more difficult. Our volunteers and patients were given only short (<1 minute) instruction on breath-hold techniques, during which end-expiratory and a relaxed position were explained.

One limitation of this study is the lack of experience with MR imagers from other manufacturers. On the MR system used in this study (Sonata; Siemens), which was equipped with a large phased-array chest coil, surface-coil inhomogeneity was limited and the fuzzy connectedness algorithm functioned excellently. For studies performed with other types of imagers, sometimes equipped with smaller surface coils, inhomogeneity artifacts may impair the performance of the algorithm (only partially, however, because of the designed underlying affinity function). This potential problem can be solved or reduced by using existing dedicated correction algorithms provided by the manufactures.

In conclusion, we have developed an algorithm to perform highly reproducible automatic measurements of the left ventricular endocardial and epicardial volumes and the associated parameters, such as myocardial mass and EF.

## References


1. Levy D, Garrison RJ, Savage DD, Kannel WB, Castelli WP. Prognostic implications of echocardiographically determined left ventricular mass in the Framingham Heart Study. N Engl J Med 1990;322:1561–1566.
2. Koren MJ, Devereux RB, Casale PN, Savage DD, Laragh JH. Relation of left ventricular mass and geometry to morbidity and mortality in uncomplicated essential hypertension. Ann Intern Med 1991;114:345–352.
3. Pattynama PM, Lamb HJ, van der Velde EA, van der Wall EE, de Roos A. Left ventricular measurements with cine and spin-echo MR imaging: a study of reproducibility with variance component analysis. Radiology 1993; 187:261–268.
4. Bellenger NG, Davies LC, Francis JM, Coats AJ, Pennell DJ. Reduction in sample size for studies of remodeling in heart failure by the use of cardiovascular magnetic resonance. J Cardiovasc Magn Reson 2000;2:271–278.
5. Fisher MR, von Schulthess GK, Higgins CB. Multiphasic cardiac magnetic resonance imaging: normal regional left ventricular wall thickening. AJR Am J Roentgenol 1985;145:27–30.
6. von Schulthess GK, Higashino SM, Higgins SS, Didier D, Fisher MR, Higgins CB. Coarctation of the aorta: MR imaging. Radiology 1986;158:469–474.
7. Higgins CB. Prediction of myocardial viability by MRI. Circulation 1999;99:727–729.
8. Holman ER, Vliegen HW, van der Geest RJ, et al. Quantitative analysis of regional left ventricular function after myocardial infarction in the pig assessed with cine magnetic resonance imaging. Magn Reson Med 1995; 34:161–169.
9. Baldy C, Douek P, Croisille P, Magnin IE, Revel D, Amiel M. Automated myocardial edge detection from breath-hold cine-MR images: evaluation of left ventricular volumes and mass. Magn Reson Imaging 1994; 12:589–598.
10. van der Geest RJ, Buller VG, Jansen E, et al. Comparison between manual and semiautomated analysis of left ventricular volume parameters from short-axis MR images. J Comput Assist Tomogr 1997;21:756–765.
11. Furber A, Balzer P, Cavaro-Menard C, et al. Experimental validation of an automated edge-detection method for a simultaneous determination of the endocardial and epicardial borders in short-axis cardiac MR images: application in normal volunteers. J Magn Reson Imaging 1998;8:1006–1014.
12. Nachtomy E, Cooperstein R, Vaturi M, Bosak E, Vered Z, Akselrod S. Automatic assessment of cardiac function from short-axis MRI: procedure and clinical evaluation. Magn Reson Imaging 1998;16:365–376.
13. Lalande A, Legrand L, Walker PM, et al. Automatic detection of left ventricular contours from cardiac cine magnetic resonance imaging using fuzzy logic. Invest Radiol 1999; 34:211–217.
14. Young AA, Cowan BR, Thrupp SF, Hedley WJ, Dell'Italia LJ. Left ventricular mass and volume: fast calculation with guide-point modeling on MR images. Radiology 2000; 216:597–602.
15. Graves MJ, Berry E, Eng AA, et al. A multicenter validation of an active contour-based left ventricular analysis technique. J Magn Reson Imaging 2000;12:232–239.
16. Barkhausen J, Ruehm SG, Goyen M, Buck T, Laub G, Debatin JF. MR evaluation of ventricular function: true fast imaging with steady-state precession versus fast low-angle shot cine MR imaging: feasibility study. Radiology 2001;219:264–269.
17. Latson LA, Powell KA, Sturm B, Schvartzman PR, White RD. Clinical validation of an automated boundary tracking algorithm on cardiac MR images. Int J Cardiovasc Imaging 2001;17:279–286.
18. Francois CJ, Fieno DS, Shors SM, Finn JP. Left ventricular mass: manual and automatic segmentation of true FISP and FLASH cine MR images in dogs and pigs. Radiology 2004; 230:389–395.
19. van der Geest RJ, Lelieveldt BP, Angelie E, et al. Evaluation of a new method for automated detection of left ventricular boundaries in time series of magnetic resonance images using an Active Appearance Motion Model. J Cardiovasc Magn Reson 2004;6: 609–617.
20. Udupa JK, Samarasekera S. Fuzzy connectedness and object definition: theory, algorithms, and applications in image segmentation. Graph Models Image Proc 1996;58: 246–261.